Supporting Information

Zhao et al. 10.1073/pnas.1105398108

SI Materials and Methods

miR-146a KO Mice. Briefly, a targeting construct where 295 base pairs of genomic sequence containing mouse premiR-146a were replaced with a floxed neomycin expression cassette was electroporated into Bruce4 ES cell line to generate miR-146a$^{-/-}$ mouse on the pure C57BL/6 background. Absence of miR-146a expression was confirmed in various hematopoietic organs by Northern blotting. Subsequent genotyping was done by duplex PCR with primers mir146a-WT-F (5′ - CTT GGA CCA GCA GTC CTC TTG ATG CAC CTT - 3′), mir146a-KO-F (5′ - ATC GCG GCC GCT TTA AGT GTA GAG AGG GGG TCA AGT A - 3′), and mir146a-R (5′ - ATT GCT CAG CGG TGC TGT CCA TCT GCA CGA - 3′) and the following PCR conditions: 94 °C for 3 min; 94 °C for 30 s, 55 °C for 30 s, 72 °C for 1 min, for 35 cycles; 72 °C for 10 min. The wild-type allele is about 900 bp and KO allele is about 700 bp.

Histology, Immunohistochemistry, and Complete Blood Count. For histological and immunohistochemical analysis, necropsied organs were fixed in 10% neutral-buffered formalin. All histology, immunohistochemistry, and complete blood count analysis were performed by the University of California, Los Angeles Pathology Research Services.

Quantitative RT-PCR. Total RNA was extracted with TRIzol reagent (Invitrogen) from total nucleated splenocytes, bone marrow cells, and CD11b^{+}-enriched splenocytes after red blood cell lysis (Biolegend). CD11b^{+} enriched splenocytes were purified by CD11b antibody-conjugated MACS beads (Miltenyi Biotec) according to the manufacturer's instructions. cDNA was synthesized using iScript cDNA synthesis kit (Bio-Rad) followed by SYBR Green-based quantitative PCR (Applied Biosystems), as previously described (1). Rpl32 level was used as the normalization.

Western Blot Analysis. Nuclear protein lysates were extracted using nuclear extraction kit (Sigma) according to the manufacturer's instructions. Antibodies against p65 (sc-8008 and sc-372), laminA/C (sc-20681), and HRP-conjugated secondary antibody (sc-2031 and sc-2004, all from Santa Cruz Biotechnology) were used for detection.

Flow Cytometry. Cells were harvested, homogenized, and red blood cells lysed with red blood cell lysis buffer (Biolegend). Fluorophore-conjugated antibodies against CD3ε, CD11b, CD19, Ter119, Gr1 (all from Biolegend) and CSF1R (Ebioscience) were used for staining. Cells were analyzed on a FACSCalibur (BD Bioscience) machine and data analysis was performed with FloJo software (Tree Star).

Statistical Analysis. All statistical analyses were performed using Prism 5 software (GraphPad). The log-rank Mantel-Cox test was used to determine statistical significance in Kaplan-Meier survival curve. The χ^2 test was used to compare tumor incidence between wild-type and miR-146a$^{-/-}$ mice and between the expected and observed distribution of offspring from p50$^{+/-}$ miR-146a$^{+/-}$ intercross. Relationship between spleen weight and percent CD11b was analyzed with correlation test. All other statistical analyses were performed with the *F*-test first to determine whether variances are different and then with the correct Student *t* test. *P* values less than 0.05 in *t* tests were considered statistically significant.

1. O'Connell RM, et al. (2008) Sustained expression of microRNA-155 in hematopoietic stem cells causes a myeloproliferative disorder. *J Exp Med* 205:585–594.

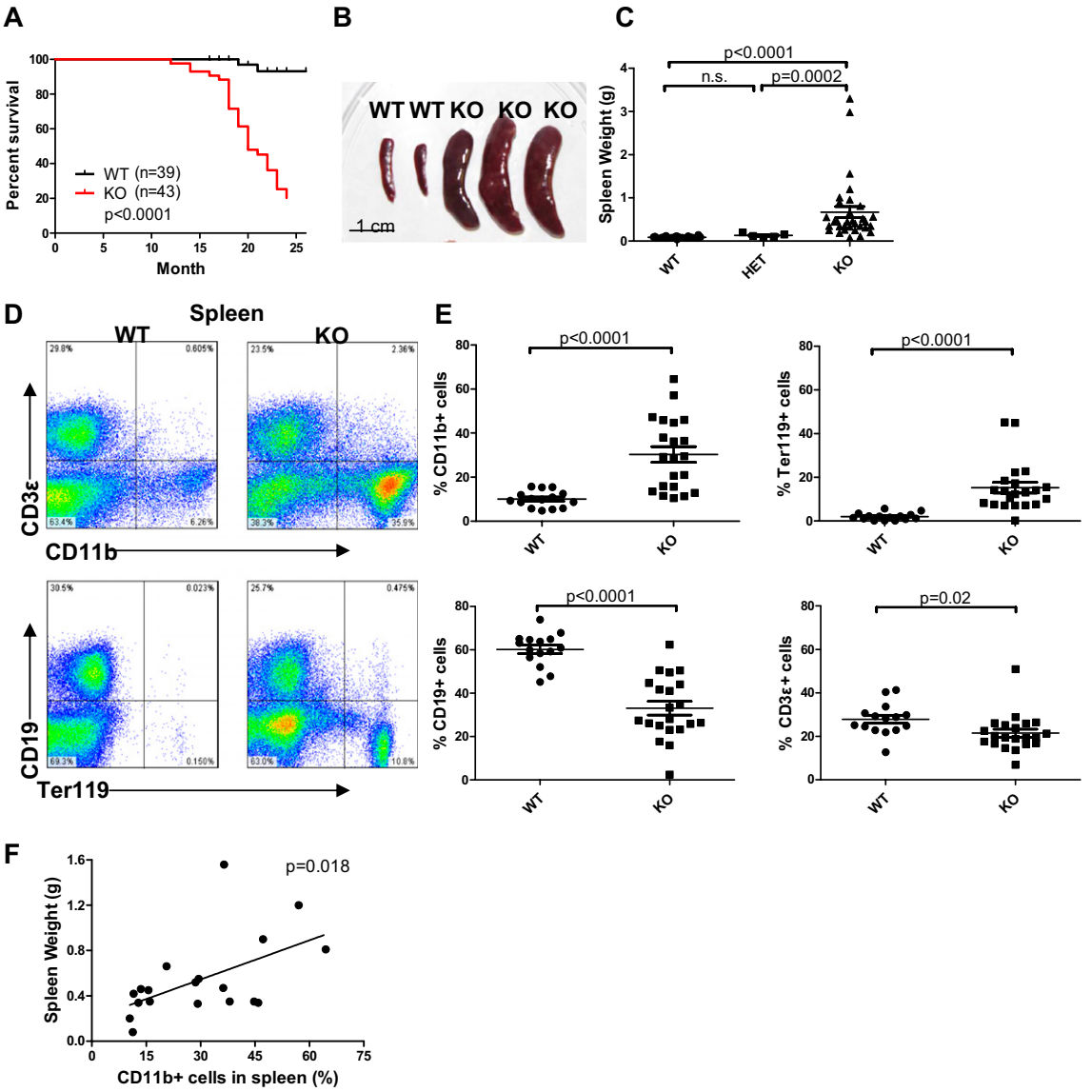

Fig. S1. miR-146a–deficient mice develop myeloproliferation in spleens. Mice were 18- to 22-mo-old miR-146a$^{-/-}$ mice (KO), miR-146a$^{+/-}$ mice (HET), and sex- and age-matched C57BL/6 control mice (WT). Data are shown as mean ± SEM. Each individual dot represents one individual mouse. At least three independent experiments were performed. (*A*) Kaplan-Meier survival curve of aging miR-146a KO and wild-type mice starting at 1 y of age (n = 39 for WT and n = 43 for KO). (*B*) Photographs of spleens isolated from KO and wild-type mice. (*C*) Weight of spleens isolated from KO, HET, and wild-type mice (n = 26 for WT, n = 5 for HET, and n = 33 for KO). (*D*) Flow cytometric analysis of nucleated splenocytes from one representative KO mouse and one representative wild-type mouse for T cells (defined as CD3ε$^+$), B cells (defined as CD19$^+$), myeloid cells (defined as CD11b$^+$), and erythroid cells (defined as Ter119$^+$). (*E*) Percentage of T cells, B cells, myeloid cells, and erythroid cells, as defined above, in nucleated splenocytes in KO and wild-type mice by flow cytometry (n = 15 for WT and n = 21 for KO from at least three independent experiments). (*F*) Correlation between spleen weight and percentage CD11b$^+$ cells in spleen from 18- to 22-mo-old miR-146a–deficient mice (n = 19).

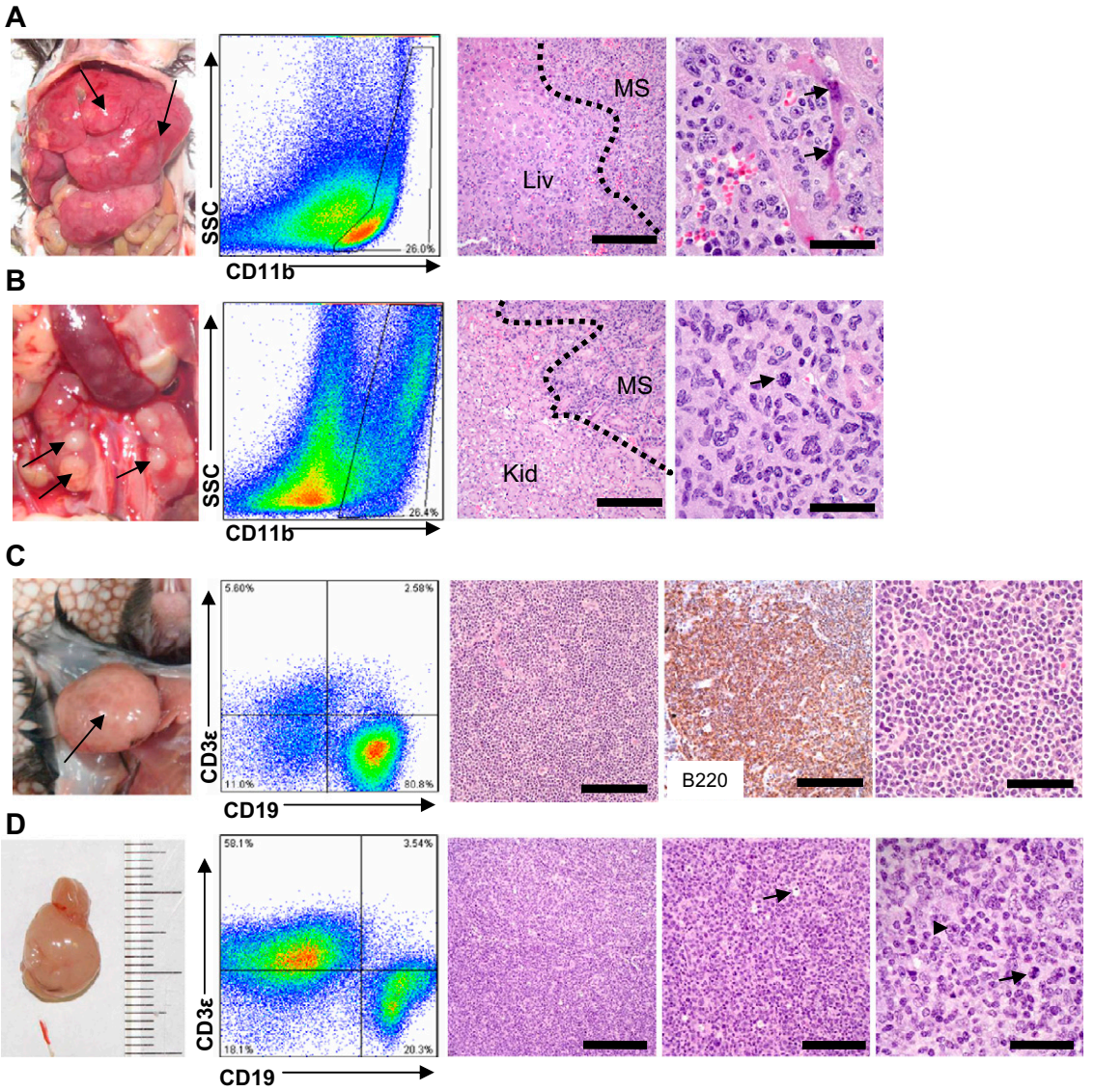

Fig. S2. Additional examples of myeloid and lymphoid malignancies in miR-146a–deficient mice. (*A*) Photograph, FACS plot, and histological analysis of a representative myeloid tumor infiltrating a KO liver. Panels 3 and 4 show an H&E-stained liver section. Liv, residual liver, MS, myeloid sarcoma infiltration. [Scale bars, (panel 3) 200 μm; (panel 4) 40 μm.] Arrows, apoptotic hepatocytes at the edge of the infiltrate. (*B*) Photograph, FACS plot, and histological analysis of a representative myeloid tumor infiltrating a KO kidney. Panels 3 and 4 show an H&E-stained kidney section. Kid, residual uninvolved kidney; MS, myeloid sarcoma infiltration. [Scale bars, (panel 3) 200 μm; (panel 4) 40 μm.] Arrow, markedly atypical mitotic figure. (*C*) Photograph, FACS plot, and histological analysis of a representative B-cell lymphoma from a KO cervical lymph node. Panels 3 and 5 show an H&E-stained spleen section. Panel 4: Positive immunohistochemical staining for B220. [Scale bar, 100 μm (panels 3 and 4); 40 μm (panel 5).] (*D*) Photograph, FACS plot, and histological analysis of a representative mixed T- and B-cell lymphoma from a KO gastrointestinal tract. Panels 3–5 show an H&E-stained tumor section. [Scale bars, (*Left* to *Right*) 200 μm, 100 μm, and 40 μm.] Arrow on panel 4, apoptotic body ("starry sky appearance"); arrowhead on panel 5, large immunoblastic cell (there are many more in this field); arrow on panel 5, atypical mitotic figure.

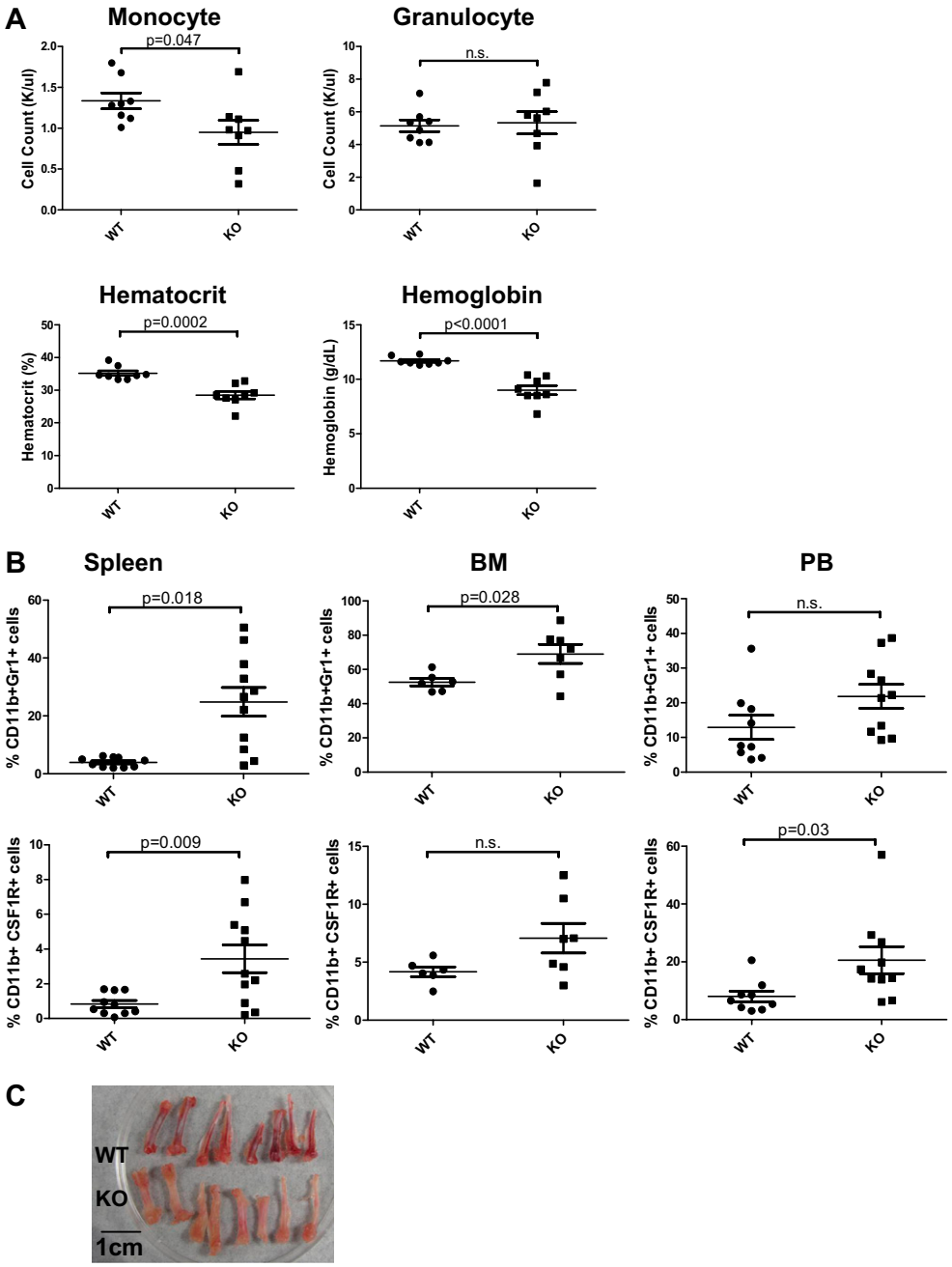

Fig. S3. Cell count and flow cytometric analysis of peripheral blood, spleen, and bone marrow. (*A*) Complete blood count of peripheral blood from 18- to 22-mo-old miR-146a$^{-/-}$ mice (KO, n = 8) and sex- and age-matched wild-type control mice (WT, n = 8). Data are shown as mean ± SEM. Each individual dot represents one individual mouse. n.s., not significant. (*B*) Percentage of CD11b/Gr1 double-positive cells and CD11b/CSF1R double-positive cells in spleen, bone marrow (BM), and peripheral blood (PB) of 18- to 22-mo-old miR-146a$^{-/-}$ mice (KO) and sex- and age-matched wild-type control mice (WT). Data are shown as mean ± SEM. Each individual dot represents one individual mouse. Total number of mice ranges from 6 to 11 from three independent experiments. n.s., not significant. (*C*) Photograph of representative tibias and fibulas isolated from wild-type or KO mice.

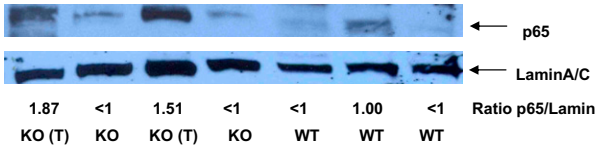

Fig. S4. Western blot analysis of the nuclear protein extracts from spleens of 18- to 22-mo-old miR-146a$^{-/-}$ mice (KO) and sex- and age-matched wild type control. KO (T), KO spleen with myeloid sarcoma; KO, KO spleen without myeloid sarcoma.

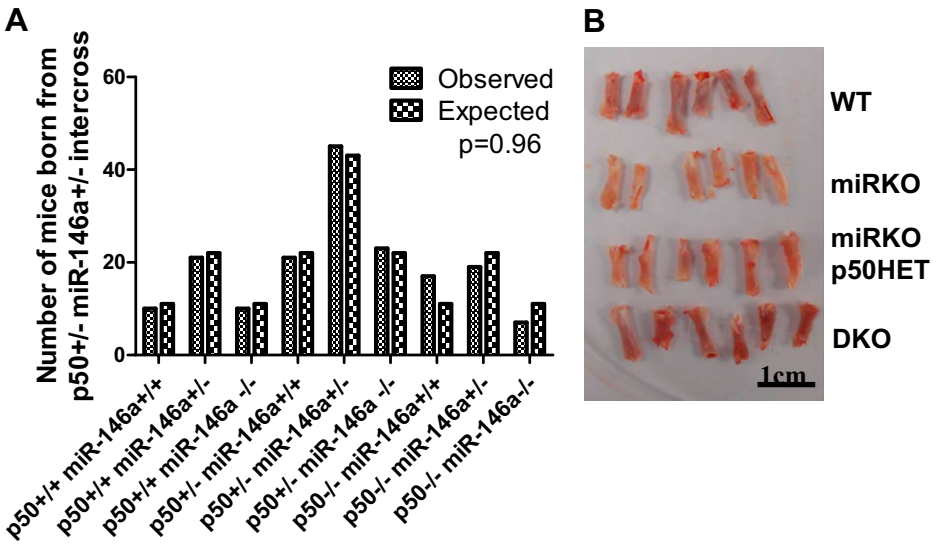

Fig. S5. (*A*) Number of offspring (n = 173) produced from $p50^{+/-}$ miR-$146a^{+/-}$ double heterozygote intercross. (*B*) Photograph of tibias from wild-type, miRKO, miRKO p50HET, and DKO mice.